Collective transport in a molecular liquid with quadrupole interaction

H. Luo and C. Hoheisel
Theoretische Chemie, Fakultät für Chemie Ruhr-Universität Bochum, Universitätsstrasse 150, 4630 Bochum, Germany
(Received 23 May 1989; revised manuscript received 18 June 1990)

With three different pair potentials we study the thermal collective transport coefficients of the N_2 model liquid by molecular-dynamics calculations. The first two of the considered pair potentials are Lennard-Jones (LJ) one-center and two-center potential functions, while the third represents a two-center LJ function plus a point-quadrupole interaction term. All three potential functions lead to acceptable transport coefficients compared with experiment. However, there appear to be significant differences in the coefficients for certain thermodynamic states. While the quadrupole interaction has only a slight effect on the time correlation functions, the two-center LJ potential influences the time correlation functions appreciably in comparison with the spherically symmetric LJ potential. The latter findings agree well with our previous results obtained for LJ liquids with four or more center potentials. On the whole, the thermal conductivity coefficient is less sensitive to the employed pair potential function than the bulk or the shear viscosity coefficient. Unfortunately there are no experimental data for the bulk viscosity.

I. INTRODUCTION

Collective transport processes in molecular liquids have only recently been studied theoretically.[1] The reason for this is twofold: (i) kinetic theory is not developed for systems of structured particles, and (ii) computer calculations are extremely expensive. Recent computations for rigid molecules have shown that reliable results for thermal transport coefficients can be obtained with present supercomputers, however, with smaller accuracy than achievable for atomic liquids.[2]

The present molecular-dynamics (MD) investigation of liquid model N_2 was undertaken to complement our knowledge of dynamic processes in molecular liquids along three different lines:

(i) which accuracy of thermal transport coefficients can be reached with common supercomputer power for a very simple molecular liquid in comparison with atomic liquids;

(ii) are the molecular transport processes largely affected by the quadrupole interaction of the molecules; and

(iii) how valuable are different potential functions for the computation of transport coefficients in comparison with experimental results and previous MD calculations for static properties.[3]

We have chosen to study liquid N_2, as bond length and the quadrupole moment of this molecule are not large. This allows us to approximate N_2 by a spherical particle. It permits us furthermore to approximate the quadrupole moment by a point-quadrupole moment. Moreover, there exist a lot of experimental transport coefficients, although not satisfactory for an exhaustive comparison. We consider nine thermodynamic states of liquid and fluid nitrogen and report also bulk viscosity coefficients, for which no experimental data are available in the literature.

II. PAIR POTENTIALS AND THERMODYNAMIC STATES

Three different pair potentials were considered for the MD computations. A spherically symmetric (one-center) Lennard-Jones (LJ) potential function of the usual form,

$$u_{\mathrm{LJ}}^{(1)}(r)=4\epsilon\left[\left[\frac{\sigma}{r}\right]^{12}-\left[\frac{\sigma}{r}\right]^{6}\right], \tag{1}$$

where σ and ϵ are the volume and strength parameters, respectively. r denotes the separation of a pair of atoms.

Second, a two-center LJ potential, which may be written as follows:

$$u_{\mathrm{LJ}}^{(2)}(r_{ij}^{\alpha\beta})=4\epsilon\sum_{i=1}^{2}\sum_{j=1}^{2}\left[\left[\frac{\sigma}{r_{ij}^{\alpha\beta}}\right]^{12}-\left[\frac{\sigma}{r_{ij}^{\alpha\beta}}\right]^{6}\right], \tag{2}$$

where σ and ϵ are now the LJ parameters for the atom-atom (site-site, center-center) interaction, and $r_{ij}^{\alpha\beta}$ denotes the separation between two interaction sites of two different molecules. The molecules are identified by α,β and the interacting centers by i,j. The number of sites per molecule is 2. Note that the separation between sites of the same molecule, the bond length d, is fixed. So the molecules are treated as rigid molecules.

Finally, a two-center LJ potential plus point-quadrupole interaction, which may be written in the following form:

$$u_{\mathrm{LJ}}^{(3)}(r_{ij}^{\alpha\beta},\mathbf{R},l_\alpha,l_\beta)=u_{\mathrm{LJ}}^{(2)}(r_{ij}^{\alpha\beta})+\frac{3}{16}\frac{Q^2}{R^5}\{1-5[(l_\alpha\cdot\mathbf{R})^2/R^2+(l_\beta\cdot\mathbf{R})^2/R^2+3(l_\alpha\cdot\mathbf{R})^2(l_\beta\cdot\mathbf{R})^2/R^4] +2[(l_\alpha\cdot l_\beta)-5(l_\alpha\cdot\mathbf{R})\cdot(l_\beta\cdot\mathbf{R})]^2\}\ , \tag{3}$$

where Q denotes the quadrupole moment of the molecule, $\mathbf{R}$ the center-of-mass (c.m.) difference position vector of two molecules α and β. l_α is a normalized vector indicating the orientation of the molecule α.

The LJ potential parametes for the three potential functions were adopted from our previous work on static properties of liquid N_2.[3] For the quadrupole moment we used the best experimental value.[4] Potential parameters and quadrupole moment are given in Table I.

We studied eight of the thermodynamic states previously considered in Ref. 3 in order to compare trends of static and dynamic quantities. Additionally the triple point state was investigated. These state points are summarized in Table II.

III. THE MOLECULAR-DYNAMICS CALCULATIONS

The MD calculations for the two-center models were performed by solving the equations of motion for translation and rotation, as described in detail elsewhere,[5] (see also the Appendix). This method of treating linear rigid models is suitable when point-quadrupole or -dipole interactions are taken into account additionally. Though the quadrupole potential function given in Eq. (3) leads to awkwardly lengthy expressions for the required pair forces, the computation speed is only slightly reduced due to the fact that the necessary orientational vectors l_α are automatically generated by the algorithm.

The equations of motion were numerically integrated by the Stoermer-Verlet algorithm, and neighbor lists were used to reduce the computation time for the evaluation of the pair forces. Some useful technical details of the MD computations are presented in Table III.

The Green-Kubo integrands for the thermal transport coefficients of a system composed of molecules can be formulated in molecule coordinates.[2] This description is particularly useful in the present case, because we perform the MD calculations in molecule coordinates (translation, rotation). Consequently, the dynamic variables, as, for example, the stress tensor, are likewise evaluated in molecule coordinates. For the heat current, we need the atomic velocities of the molecule centers rather than the c.m. velocities. However, the former can easily be obtained by the angular and c.m. velocities.

TABLE I. Pair potential parameters used for the description of the pair interaction in the liquid N_2.

Type	σ (Å)	ϵ/k_B (K)	d (Å)	$10^{26}\ Q$ (esu)
$u_{\mathrm{LJ}}^{(1)}$	3.6360	101.6		
$u_{\mathrm{LJ}}^{(2)}$	3.2932	36.5	1.094	
$u_{\mathrm{LJ}}^{(3)}$	3.3140	35.3	1.101	1.52

We give a useful comparison of computation speeds, which arise through the use of different MD computation methods, in the Appendix.

A further point of interest should perhaps be mentioned. The calculations based on the two-center LJ potential including quadrupole moment require at least systems of 108 molecules to guarantee a sufficiently long cutoff radius for the potential.

IV. RESULTS

A. Time correlation functions

1. *States far off the experimental triple point of N_2*

For two states outside the neighborhood of the triple point of N_2 we illustrate the computed time correlation functions of the nondiagonal part of the stress tensor and the heat current in Figs. 1–4. The figures contain results for the one- and the two-center potentials as well as for the two-center potential with quadrupole interaction. Evidently, the Green-Kubo integrands calculated with the one-center LJ potential differ essentially from those obtained with the other potentials. However, the quadrupole interaction changes the correlation functions (CF's) only slightly.

The remarkably different time behavior of the CF's in atomic and molecular liquids has been observed previously in MD studies of globular molecules.[2] For liquid N_2, these differences are particularly interesting, as the integrals over the CF's give equal transport coefficients within the statistical uncertainties.

From our knowledge of the slight influence of the quadrupole interaction on static properties of liquid model N_2 (Refs. 3 and 6), we expected no large effect of the quadrupole moment on the collective dynamic processes. The small differences in the time CF's at low-pressure states can be explained by the predominant occurrence of T-shaped molecule configurations, when quadrupole in-

TABLE II. Thermodynamic states of liquid and fluid N_2 considered for the computations.

State point	ρ (g cm^{-3})	T (K)	Comment
1	0.7003	100	
2	0.7003	150	
3	0.7003	250	
4	0.7003	400	
5	0.8678	63	triple point
6	0.8684	70	
7	0.8684	100	
8	0.8684	150	
9	0.8686	250	

TABLE III. Technical details of the molecular-dynamics computations.

Number of molecules N	108 (32)
Number of atomic centers	216 (64)
Ensemble	NVEp
	V volume, E total energy,
	p total momentum
Integration algorithm	Stoermer-Verlet
Integration time step	0.5×10^{-14} s
Starting configuration	liquidlike
Equilibration runs	1000 steps
Production runs	10^5 steps
Computation times	
for 1000 steps	6.0 s ($u_{LJ}^{(1)}$)
with 108 molecules (Cyber 205)	27.8 s ($u_{LJ}^{(2)}$)
	37.3 s ($u_{LJ}^{(3)}$)
Cutoff radius for the LJ potentials	2.55σ

teraction is present. Occurrence of T-shaped structures is favored by low pressures. Apparently, T-shaped configurations support long-lived dynamic correlations reflected in the tail behavior of the CF's plotted in Fig. 1.

2. *Triple point state of N_2*

The time CF for the heat current shows rapid decay independent of the state investigated. However the CF's for the shear viscosity η_s and the bulk viscosity η_v display a significant long-time behavior in the sense that positive correlations persist up to about 3 ps. The plots in Figs. 5 and 6 illustrate this microscopic long-time behavior of the Green-Kubo integrands for the three potential functions employed.

Microscopic tails are expected for the CF's for η_s and η_v near the liquid-solid phase transition. For atomic liquids, the tails are well known by computer calculations (see Ref. 7).

For the present case of N_2, three potentials $u_{LJ}^{(1)}-u_{LJ}^{(3)}$ lead to a rather good description of the triple point of N_2 (state 5). However, the spherically symmetric potential is somewhat inferior. It generates a too slowly decaying CF resulting in a too large shear viscosity coefficient. We see furthermore from Figs. 5 and 6 that the CF's obtained with the quadrupole interaction show stronger correlations in the range of 0.2–1.0 ps. This confirms what we have discussed in Sec. IV A 1.

B. The transport coefficients of liquid N_2

Shear, bulk viscosity and thermal conductivitiy coefficients computed by MD with the three potentials presented in Sec. II are summarized in Table IV. Statistical errors are indicated and values computed with 32 rather than 108 molecules are given in brackets. A detailed investigation of the molecule number dependence of the results will be reported in a forthcoming paper.[8] The table contains also experimental transport

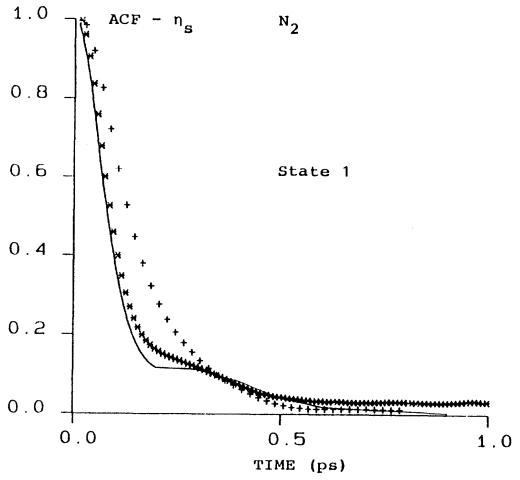

FIG. 1. Normalized Green-Kubo integrands for η_s computed by MD with three potentials: $+++$, $u_{LJ}^{(1)}$; ---, $u_{LJ}^{(2)}$; $***$, $u_{LJ}^{(3)}$. State point 1.

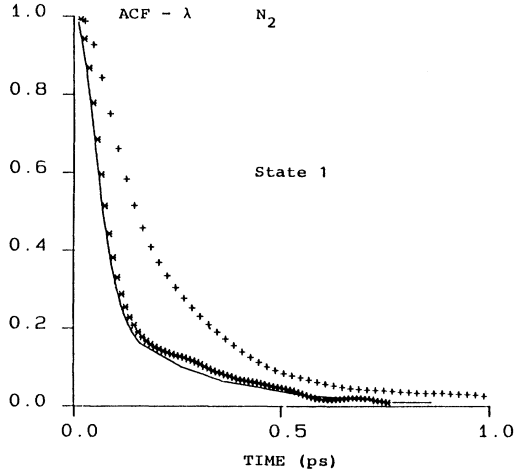

FIG. 2. Same as in Fig. 1, but for λ.

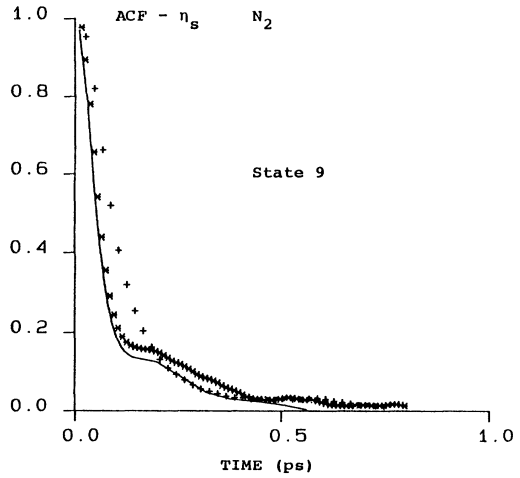

FIG. 3. Same as in Fig. 1, but for state point 9.

coefficients for comparison. Bulk viscosity does not seem to have been measured for N_2.

We shall discuss the results separately for the transport coefficients in the following sections.

1. Shear viscosity η_s

For the low-pressure states, 1, 5, and 6, the one-center LJ potential generates significantly higher shear viscosities than the molecular potentials. The latter give better agreement with the experimental values, although for the triple point state the predicted η_s values are too small. For the triple point we expect, however, a molecule number dependence of η_s leading to a slightly higher value for larger systems.[7] Quadrupole interaction enlarges slightly the shear viscosity and gives better agreement with experiment.

For the high-pressure states, 2–4 and 7–9, particularly at higher density, the spherically symmetric potential generates too high η_s values compared with experiment. This indicates deficiencies of the simplified potential model. Both molecular potential functions give good agreement with experiment, although the quadrupole interaction does not improve agreement in these instances.

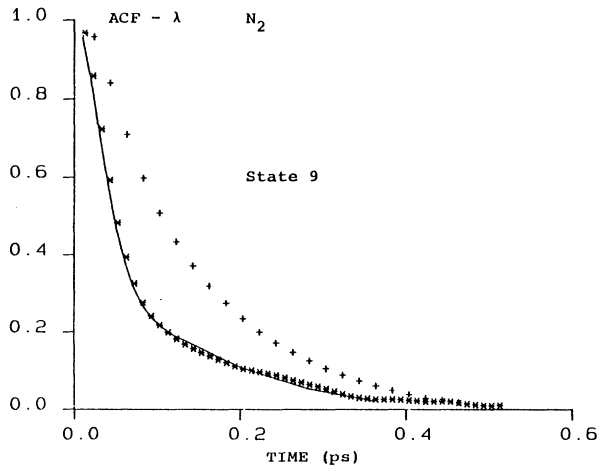

FIG. 4. Same as in Fig. 1, but for λ and state point 9.

2. Thermal conductivity λ

For the thermal conductivity λ, all the three-potential functions generate comparable values at low- and high-pressure states. The agreement with experiment is good for states, where we know accurate experimental numbers. In order to compare our computed λ values with experimental values also for high-pressure states we have extrapolated existing λ values measured at low pressure to the range of high pressures. On the whole a small tendency of the computed λ values to lie below the experimental ones is noticeable.

On the other hand, the thermal conductivity seems to be rather insensitive to potential variations in MD calculations, since the three employed potentials cause no systematic changes of this quantity.

3. Bulk viscosity η_v

The bulk viscosity coefficient depends more strongly on the choice of the potential than the other transport coefficients. While the one-center LJ potential generates the lowest values, the two-center LJ plus quadrupole interaction gives the highest values. As we have no experimental data to compare with, it is difficult to assess which potential predicts the most realistic η_v values. We believe that the rather large differences presented in Table IV are partly due to molecule number effects. The Green-Kubo integrand for η_v involves the PV term, where P denotes the pressure and V the volume of the microcanonical ensemble considered (see, for example, Ref. 7). An accurate determination of this PV term requires larger molecule numbers for the MD computations than we have used here. So for η_v our results contain a systematic uncertainty not indicated in the table. We shall, however, compute η_v more accurately in a separate paper, where the molecule number dependence of this transport coefficient is considered.[8]

V. DISCUSSION AND CONCLUSIONS

Before we summarize our results, a few essential comments on the accuracy of the computed transport coefficients are in order.

On inspecting the graphs of the autocorrelation functions (ACF's) in Figs. 5 and 6 one realizes that these functions have not completely disappeared within the displayed time range. So one might think that the omitted part of these functions could substantially contribute to the time integral and thus to the transport coefficient. We have examined this point carefully. First, the presented ACF's were obtained from a single run each, while at least three runs were used to determine the transport coefficient. Secondly, the plotted time range is indeed sufficient for the integration to give all the transport coefficients except the bulk viscosity with the given

accuracy. We have ensured this by test integrations of the various ACF's up to several picoseconds.

For states above the triple point the ACF's decay very quickly and integration is no problem. We found that integration of the η_s, η_v, and λ Green-Kubo integrands until 1.2 ps always gives reliable results.

For states near the triple point, the integration has to be extended to a few picosecods to guarantee a reliable result for the transport coefficient. An exception is the bulk viscosity, for which longer runs and larger molecule numbers are necessary.

To illustrate the dependence of the transport coefficients η_s and η_v on the integration time of the relevant Green-Kubo integrands near the triple point state, we have performed complementary runs with 256 molecules and 10^5 time steps with use of the two-center LJ potential. The results are summarized in Table V. They confirm our above statements. The correlation functions obtained by these runs are hardly distinguishable from those plotted in Figs. 5 and 6. However, the bulk viscosity value displayed in Table V has a smaller error bar than the value presented in Table IV due to the larger system used for the runs.

The question of the system size dependence of the results is only relevant for states near the triple point. For the triple point, all our computations based on the molecular potentials showed insignificant molecule number dependence of both the ACF's and the transport coefficients, apart from η_v. An exhaustive study will be published later.[8]

TABLE IV. Thermal transport coefficients of liquid N_2 obtained from MD computations and experiment. The rows given per state have the order: first, from the one-center LJ potential; second, from the two-center LJ potential; third, from the two-center LJ potential plus quadrupole interaction; fourth, from experiment (Ref. 9). Values obtained by computations with 32 molecules are given in brackets.

State	$10^4\eta_s$ (Pa s)	$10^4\eta_v$ (Pa s)	$10^3\lambda$ (mW m^{-1} K^{-1})	Comment
1	0.825±0.04	0.538±0.03	86.5±4	
	0.725±0.03	0.805±0.06	81.0±4	(η_s:0.762; η_v:0.931; λ=78.2)
	0.757±0.03	0.900±0.06	85.3±4	
	0.76±0.05		100±10	
2	0.844±0.04	0.411±0.03	95.1±4	
	0.759±0.04	0.635±0.05	95.1±4	
	0.746±0.04	0.758±0.06	95.1±4	
	0.72±0.5		100.0±20	
3	0.856±0.05	0.319±0.02	101.9±5	high-pressure states
	0.844±0.05	0.626±0.06	103.8±5	
	0.67±0.05			
4	0.865±0.05	0.373±0.02	117.9±5	
	0.874±0.06	0.738±0.08	118.4±5	
	0.60±0.05			
5	3.22±0.3	1.29±0.1	141.0±5	triple point state
	2.02±0.2	1.40±0.2		
	2.27±0.2	1.79±0.2	140.5±10	
	2.90±0.1		156.0±5	
6	2.59±0.1	0.85±0.05	144.1±7	
	1.91±0.1	0.90±0.2	142.8±7	
	2.15±0.1	1.84±0.3	142.3±7	
	2.20±0.1		149.5±5	
7	2.12±0.1	0.621±0.05	146.1±7	
	1.59±0.1	0.778±0.08	157.5±7	
	1.74±0.1	1.34±0.2	164.0±8	
	1.50±0.2		180.0±20	
8	1.93±0.1	0.563±0.05	168.0±8	
	1.73±0.1	0.802±0.08	161.5±8	high-pressure states
	1.74±0.1	1.33±0.2	167.8±8	
	1.15±0.2			
9	1.69±0.1	0.476±0.05	175.2±8	
	1.50±0.1	0.932±0.08	179.1±8	
	1.70±0.1	1.06±0.1	191.0±10	
	0.90±0.2			

TABLE V. Shear bulk viscosity coefficients (in units of 10^{-4} Pa s), dependent on the integration time of the Green-Kubo integrands.

Integration time (ps)	Run 1		Run 2		Run 3	
	η_s	η_v	η_s	η_v	η_s	η_v
3.0	2.15	1.10	1.86	1.10	2.12	1.22
3.5	2.14	1.06	1.91	1.13	2.17	1.23
4.0	2.09	1.08	1.96	1.12	2.20	1.24
4.5	2.07	1.09	1.98	1.11	2.24	1.27
5.0	2.01	1.13	2.00	1.20	2.26	1.28

Our calculations with the one-center LJ potential are subjected to particle number effects. The latter effects are discussed at length in Ref. 7. The error bars given for the latter results account, however, for these systematic uncertainties.

Our computations show that the collective transport coefficients of liquid and fluid N_2 can be determined in rather good agreement with experiment using the proposed three potential functions $u_{LJ}^{(1)}$, $u_{LJ}^{(2)}$, and $u_{LJ}^{(3)}$. The overall agreement is better when the molecular potentials $u_{LJ}^{(2)}$ and $u_{LJ}^{(3)}$ are employed. However, the spherically symmetric potential also gives useful values. The quadrupole interaction has only a slight effect on the correlation functions and the transport coefficients. In most cases, the quadrupole interactions lead, however, to an improvement of the transport coefficients compared with experiment.

Very sensitive to the form of the potential is the bulk viscosity coefficient, while the thermal conductivity coefficient is practically independent of which of the three potentials is employed.

According to previous findings, the molecule number dependence of the results is small, even in the region near the triple point. An exception is the bulk viscosity, for which calculations with larger molecule number are required, when Lennard-Jones type potentials are applied. This problem is well known from computations for atomic liquids[10] and will be treated in forthcoming publications.

Our results for the thermal transport coefficients support the tendencies discovered in a previous work on static properties of N_2.[3] For the dynamic processes, the inclusion of the quadrupole interaction is, however, more important than for thermodynamic quantities.

ACKNOWLEDGMENTS

The Rechenzentrum der Ruhr-Universität Bochum generously allocated computation time on the Cyber 205 vector machine, and the Deutsche Forschungsgemeinschaft gave financial support (Grant No. Ho 626/13-1).

APPENDIX

The determination of thermal transport coefficients via the Green-Kubo method requires the correlation function of the desired dynamic variable. For a system of atoms as well as molecules, the evaluation of the thermal con-

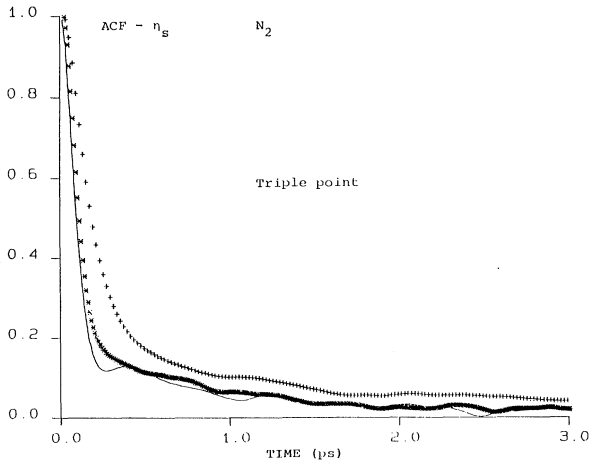

FIG. 5. Same as in Fig. 1, but for the triple point (state 5).

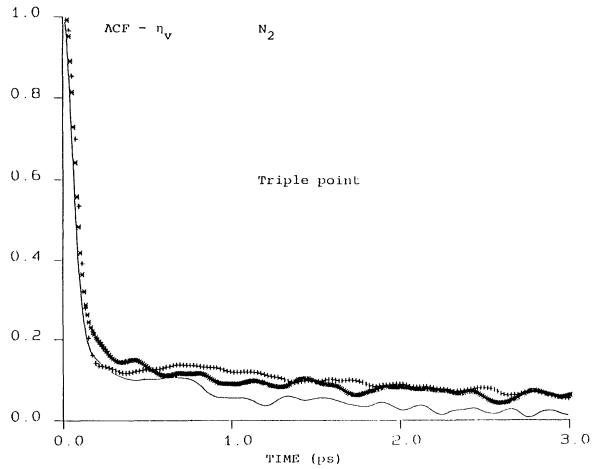

FIG. 6. Same as in Fig. 1, but for η_v and the triple point (state 5).

TABLE VI. Comparison of computation times using the present and the constraints MD method for the computation of the stress tensor elements and the microscopic heat current with potential $u_{\mathrm{LJ}}^{(2)}$.

MD method	Computation time on the Cyber 205 for 1000 time steps	Number of molecules
Present	7.4	32
	27.8	108
Constraints	7.6	32
	35.9	108

ductivity λ involves by far the most expansive computations. So we consider this case here for a system of linear rigid molecules. The Green-Kubo integral then reads

$$\lambda=\frac{1}{3Vk_BT^2}\int_0^\infty \langle \mathbf{J}_q(o)\cdot\mathbf{J}_q(t)\rangle dt \ ,$$

where $\mathbf{J}_q(t)$ denotes the heat flux, V the volume, T the temperature, and k_B the Boltzmann constant. The brackets indicate the thermal average over the chosen ensemble, here the microcanonical one. $\mathbf{J}_q(t)$ is decomposable into a kinetic and a potential contribution:

$$\mathbf{J}_q(t)=\mathbf{J}_k(t)+\mathbf{J}_p(t) \ ,$$

where

$$\mathbf{J}_k=\frac{M}{2}\sum_{\alpha=1}^{N}\dot{\mathbf{R}}_\alpha^2\dot{\mathbf{R}}_\alpha \ ,$$

$$\mathbf{J}_p=-\tfrac{1}{2}\sum_{\alpha=1}^{N}\sum_{i=1}^{2}\dot{\mathbf{r}}_\alpha^i\sum_{\beta\neq\alpha}^{N}\sum_{j=1}^{2}\left[\mathbf{R}_{\alpha\beta}\frac{\partial u(r_{\alpha\beta}^{ij})}{\partial \mathbf{r}_{\alpha\beta}^{ij}}-u(r_{\alpha\beta}^{ij})\mathsf{i}\right] .$$

We have thereby used the following notation: M is the mass of the molecule, $\mathbf{R}$ the position vector of the c.m. of the molecule α, and $\mathbf{R}_{\alpha\beta}$ the difference vector between the c.m. positions of pairs of molecules α,β. $u(r_{\alpha\beta}^{ij})$ is the atomic pair potential function depending on the separation between interaction centers of different molecules α,β. $\mathbf{r}_\alpha^i$ is the position vector of the interaction center α, and $\mathbf{r}_{\alpha\beta}^{ij}$ the difference between position vectors of centers i,j of different molecules α,β. N is the molecule number and i the unit tensor indicating that the whole expression in large parentheses is to be evaluated as a tensor. Time dependence of the relevant coordinates have been left out in the above notation, for shortness.

Using the present MD method with separate c.m. and rotational coordinates the evaluation of $\mathbf{J}_k$ and $\mathbf{J}_q$ is straightforward, as the necessary quantities are directly computed in the integration algorithm.[5]

However, application of the constraints method[11] for the MD requires additional calculation of the molecule coordinates $\mathbf{R}_\alpha$ or $\mathbf{R}_\beta$. In particular, the projection of the forces on the molecular separation vector occurring in the tensor expression requires additional computation effort. As a result, the computation times of the constraints method exceed those of the present method, particularly for larger molecule numbers.

We compare computation times of both MD methods for the evaluation of the stress-tensor elements and the heat flux with potential $u_{\mathrm{LJ}}^{(2)}$ in Table VI.

[1]D. J. Evans and W. B. Streett, Mol. Phys. **36**, 161 (1978); G. Marechal, J.-P. Ryckaert, and A. Bellemans, *ibid.* **61**, 33 (1987); R. Edberg, G. P. Morriss, and D. J. Evans, J. Chem. Phys. **86**, 4555 (1987).
[2]C. Hoheisel, J. Chem. Phys. **89**, 3195 (1988).
[3]R. Vogelsang and C. Hoheisel, Phys. Chem. Liq. **16**, 189 (1987).
[4]C. G. Gray and K. E. Gubbins, *Theory of Molecular Fluids* (Clarendon, Oxford, 1984), Vol. 1.
[5]C. Hoheisel, R. Vogelsang, and M. Schoen, Comput. Phys. Commun. **43**, 217 (1987).
[6]P. S. Chung and J. G. Powles, Mol. Phys. **30**, 1983 (1976).
[7]C. Hoheisel and R. Vogelsang, Comput. Phys. Rep. **8**, 1 (1988).
[8]H. Luo and C. Hoheisel, J. Chem. Phys. (to be published).
[9]*Zahlenwerte und Funktionen,* Vols. IV–VI of *Landolt-Börnstein* (Springer, Berlin, 1969).
[10]C. Hoheisel, R. Vogelsang, and M. Schoen, J. Chem. Phys. **87**, 7195 (1987).
[11]G. Ciccotti and J.-P. Ryckaert, Comput. Phys. Rep. **4**, 345 (1986).